

A STATICALLY CONDENSABLE ENRICHMENT FOR PRESSURE DISCONTINUITIES IN TWO-PHASE FLOWS

Roberto F. Ausas^a, Gustavo C. Buscaglia^a and Sergio R. Idelsohn^b

^a*Instituto de Ciências Matemáticas e Computação, Universidade de São Paulo, Av. do Trabalhador
São-carlense 400, 13560-970 São Carlos, SP, Brazil, rfausas@gmail.com*

^b*Centro Internacional de Métodos Numéricos en Ingeniería., Edificio C1, Campus Norte UPC C/ Gran
Capitán S/N 08034 Barcelona, España, sergio@cimne.upc.edu*

Keywords: Finite elements, Discontinuous pressures, Enrichment function, Static condensation.

Abstract. We introduce a new finite element space for discontinuous pressures at immersed boundaries not conforming with the mesh. The proposed space incorporates two additional degrees of freedom that are local to the elements crossed by the interface, linear on each side, discontinuous at the interface and zero at the element nodes. The new degrees of freedom can be statically condensed before final assembly, therefore avoiding difficulties associated with the update of the mesh graph in the case of moving interfaces as happens for instance with the well known extended finite element method (XFEM). The implementation of the new space in any existing finite element code is extremely easy in two and three spatial dimensions, since the new shape functions are based on the usual P1 functions. The new space is compared with the classical P1-conforming space and with another finite element space without additional unknowns also proposed by the authors (see Ausas, Simeoni and Buscaglia, *Comput. Meth. Appl. Mech. Engng.*, 2010) in several problems involving jumps in the viscosity and in the presence of singular forces, in two dimensions and in more challenging three dimensional situations. Based on the numerical experiments we show that the behavior of the new space is equal or better than that of the aforementioned space.

1 INTRODUCTION

Simulation of free-surface and/or two-phase flows is still a challenge in computational fluid dynamics because neither the shape nor the positions of the interfaces are known a priori. These problems can be solved using the interface-tracking or the interface-capturing methods. The former computes the motion of the fluid particles using a Lagrangian approach and the computational domain adapts to the shape of the interface (see for instance [Hughes et al. \(1981\)](#); [Hirt et al. \(1974\)](#); [Cruchaga et al. \(2001\)](#); [Dettmer et al. \(2003\)](#); [Baiges et al. \(2010\)](#)). A different approach for the simulation of free-surface flows that is based on Lagrangian particles can be found in [Idelsohn et al. \(2004, 2009\)](#). On the other hand, in the front-tracking method [Unverdi and Tryggvason \(1992\)](#); [Gueyffier et al. \(1999\)](#); [Popinet and Zaleski \(1999\)](#), the interface is represented by a surface mesh advected with a Lagrangian method while immersed in an Eulerian (fix) mesh where the flow problem is solved considering the fluids as a single fluid with variable properties.

The other alternative are the interface-capturing methods like the Volume-of-fluid technique (see [Hirt and Nichols \(1981\)](#); [Kothe et al. \(1996\)](#); [Cummins et al. \(2005\)](#)) and the level set method (see for example [Adalsteinsson and Sethian \(1995\)](#); [Sethian \(2001\)](#); [Osher and Fedkiw \(2001\)](#)). The flow problem is solved in a fixed mesh considering a single fluid with variable properties. Variants of these methods differ in two aspects: first, the technique used to solve the transport equation for the scalar function used to represent the interface, for which several schemes have been proposed (see [Shu and Osher \(1988\)](#); [Jiang and Peng \(2000\)](#); [Sweby \(1984\)](#); [Enright et al. \(2002\)](#); [Marchandise et al. \(2006\)](#); [Di Pietro et al. \(2006\)](#) for purely Eulerian methods and [Enright et al. \(2005\)](#); [Strain \(1999a,b\)](#) for semi-Lagrangian methods). The other differences are related to the method used to solve the Navier-Stokes equations for a one phase flow with variable properties and in how the discontinuities and kinks in velocity and pressure that may arise at the interface due to discontinuities in the physical properties and/or the presence of singular force are approximated.

Several remedies have been proposed to improve accuracy and robustness of computations in Eulerian formulations. For instance, in [Brackbill et al. \(1992\)](#) a treatment of the singular forces at the interface by means of a regularization is proposed, such that, sharp variations in the pressure field are avoided. In [Löhner et al. \(2006\)](#) and [Carrica et al. \(2007\)](#), different extrapolation techniques of the velocity and pressure near the interface are presented. In [Ausas and Buscaglia \(2010\)](#) a velocity extrapolation method is also discussed.

In this work we focus the attention on how to improve the accuracy of simulations in finite element formulations by means of improving the approximation spaces. In this case, since a partition of the computational domain into simplices is made and the interface does not necessarily conform with the element edges, standard finite element methods, either continuous or discontinuous across inter-element boundaries, suffer from suboptimal approximation orders. Poor approximation orders cause spurious velocities near the interface that may affect accuracy and robustness of simulations as described for instance in [Ganesan et al. \(2007\)](#). One possibility is to locally modify the finite element spaces in those elements cut by the interface in order to accommodate the discontinuities. This can be done without introducing additional degrees of freedom as shown by Ausas et al [Ausas et al. \(2010a\)](#) in which a new finite element space has been introduced. The interpolation properties of this space are discussed thoroughly in [Buscaglia and Agouzal \(2011\)](#). When taken as pressure space, the accuracy of Navier-Stokes computations in equal-order velocity-pressure approximations is not limited, since the global accuracy is already limited by the $H^1(\Omega)$ -accuracy of the velocity space, which is at most $\mathcal{O}(h)$.

Another option is to add degrees of freedom or enrich the finite element spaces at the elements cut by the interface. Minev and co workers [Minev et al. \(2003\)](#) use gradient velocity shape functions and discontinuous pressure shape functions also for problems involving surface tension. Also, for two-phase flow problems, Chessa and Belytschko [Chessa and Belytschko \(2003\)](#) use an enrichment method called XFEM, initially developed by the second author for the modeling of cracks [Belytschko et al. \(2001\)](#). Both approaches lead to optimal orders of convergence, but the main drawback is that the additional degrees of freedom cannot be eliminated before assembly. The connectivity of the unknowns depend on the position of the interface, therefore the mesh graph needs to be updated as the interface moves. Also, it has been observed that the resulting linear system becomes ill-conditioned and that the linear independence of the finite element basis deteriorates as the mesh size is reduced. This XFEM approach has also been used recently in [Gross and Reusken \(2007b,a\)](#); [Reusken \(2008\)](#) for two-phase flows. Another method that is related to the XFEM approach, but avoids the inclusion of additional degrees of freedom is presented by Fries et al [Fries and Belytschko \(2006\)](#), but some complexities related to the moving least square approach used have to be dealt with. Also, in [Coppola-Owen and Codina \(2005\)](#), Codina and Coppola introduce an enrichment for the treatment of kinks in the pressure field as typically happens in problems with jumps in the density in the presence of a gravitational field. The additional degree of freedom can be statically condensed prior to assembly.

In this paper a new enrichment space for discontinuous pressures is proposed. Two enrichment functions are introduced at the elements cut by the interface. The additional functions are local to each element, linear on each side of the interface, discontinuous just at the interface and zero at the element nodes. The new degrees of freedom can be statically condensed prior to assembly, thus avoiding difficulties related with the update of the mesh graph. Implementation of this enrichment in existing finite element programs results easy regardless the number of spatial dimensions, since the new shape functions can be computed using the classical P_1 functions. As revealed in the numerical experiments, the interpolation properties of this enrichment space are equal or better than those of the space presented in [Ausas et al. \(2010a\)](#).

The plan of the article is the following: after this introduction, the mathematical problem and jump conditions in two-phase flows are presented. Also, the continuous and discrete variational formulations are written. Next, the new enrichment space for discontinuous pressures is explained with details to construct the enrichment basis functions. In section 4 several test examples in two dimensions are shown. Finally, some conclusions are drawn.

2 GOVERNING EQUATIONS

We consider the incompressible Navier–Stokes equations. Let Ω be a domain in \mathbb{R}^d ($d = 2$ or 3). The problem is to find a velocity field \mathbf{u} and a pressure field p such that

$$\rho \left(\frac{\partial \mathbf{u}}{\partial t} + \mathbf{u} \cdot \nabla \mathbf{u} \right) - \nabla \cdot (2\mu \nabla^S \mathbf{u}) + \nabla p = \rho \mathbf{b} \quad \text{in } \Omega, t > 0, \quad (1)$$

$$\nabla \cdot \mathbf{u} = 0 \quad \text{in } \Omega, t > 0, \quad (2)$$

$$\mathbf{u} = \mathbf{u}_{\partial\Omega} \quad \text{in } \partial\Omega, t > 0, \quad (3)$$

$$\mathbf{u} = \mathbf{u}_0 \quad \text{in } \Omega, t = 0, \quad (4)$$

where \mathbf{b} is a volume force, $\mathbf{u}_{\partial\Omega}$ are the Dirichlet boundary conditions and \mathbf{u}_0 is the initial condition for the velocity field. We restrict to the case of two phase flows. The domain Ω is divided into subdomains Ω^+ and Ω^- . The fluid properties (density and viscosity) are then given by

$$(\rho(\mathbf{x}), \mu(\mathbf{x})) = \begin{cases} (\rho^+, \mu^+) & \text{if } \mathbf{x} \in \Omega^+ \\ (\rho^-, \mu^-) & \text{if } \mathbf{x} \in \Omega^- \end{cases} \quad (5)$$

The fluid domains Ω^+ and Ω^- are separated by an interface denoted by $\Gamma = \Omega^+ \cap \Omega^-$. We recall here the boundary or jump conditions at this internal interface.

Jump conditions for a Newtonian fluid

The standard jump conditions at internal boundaries are briefly recalled here. In the first place, the velocity field at the interface \mathbf{u} is decomposed into its normal and tangential parts as follows

$$\mathbf{u} = u_n \mathbf{n} + \mathbf{u}_s, \quad (6)$$

where $u_n = \mathbf{u} \cdot \mathbf{n}$. The interface forces must balance the sum of the forces exerted on Γ from the “positive” side, plus those from the “negative” side. This is expressed as

$$(\sigma^- - \sigma^+) \cdot \mathbf{n} = \mathbf{f}_\Gamma. \quad (7)$$

We are interested in the *normal component* of this jump that reads

$$[(\sigma^- - \sigma^+) \cdot \mathbf{n}] \cdot \mathbf{n} = \llbracket \sigma_{nn} \rrbracket = \llbracket -p + 2\mu \frac{\partial u_n}{\partial n} \rrbracket = f_{\Gamma n}. \quad (8)$$

Remark: In the general case, both the pressure and the velocity gradient can be discontinuous at the interface. However, for problems involving surface tension, in the absence of Marangoni or thermocapillary effects, the force \mathbf{f}_Γ is normal to the interface and given by

$$\mathbf{f}_\Gamma = \gamma \kappa \mathbf{n}, \quad (9)$$

where γ is the (constant) surface tension coefficient and κ is the mean curvature of the interface. If viscosities of both fluids are the same, just the pressure exhibits a jump. In the numerical solution of problem (1)–(4) with the jump conditions (8), regardless of the method used, be it finite elements or finite differences, special care has to be taken to accommodate the discontinuities in the fluid–dynamical variables near the interface. In this article we use a finite element method of which the variational formulation is presented below. In this case, the key issue relies in how to choose the approximation spaces for pressure and velocity.

2.1 Variational formulations

The variational formulation for the problem to be solved is

Find $(\mathbf{u}, p) \in V \times Q$ such that

$$\int_{\Omega} \rho \left(\frac{\partial \mathbf{u}}{\partial t} + \mathbf{u} \cdot \nabla \mathbf{u} \right) \cdot \mathbf{v} \, d\Omega + \int_{\Omega} 2\mu D\mathbf{u} : D\mathbf{v} \, d\Omega - \int_{\Omega} p \nabla \cdot \mathbf{v} \, d\Omega = \int_{\Omega} \mathbf{b} \cdot \mathbf{v} \, d\Omega + \mathbf{f}_{\Gamma}(\mathbf{v}) \quad (10)$$

$$\int_{\Omega} q \nabla \cdot \mathbf{u} \, d\Omega = 0 \quad (11)$$

$\forall (\mathbf{v}, q) \in V \times Q$. The term $\mathbf{f}_{\Gamma}(\mathbf{v})$ accounts for a singular force concentrated at Γ . For the case of surface tension we use a Laplace–Beltrami formulation (see e.g. [Bänsch \(2001\)](#); [Ganesan et al. \(2007\)](#); [Gross and Reusken \(2007b\)](#))

$$\mathbf{f}_{\Gamma}(\mathbf{v}) = - \int_{\Gamma} \gamma(\mathbf{x}) (\mathbb{I} - \mathbf{n} \otimes \mathbf{n}) : \nabla \mathbf{v} \, d\Gamma, \quad (12)$$

accounting for the surface tension force and Marangoni effects.

We use a stabilized formulation based on the ASGS (Algebraic Subgrid Scale) method for discretization (see e.g. [Codina \(2001\)](#) and references therein) together with a trapezoidal rule for temporal discretization and a monolithic approach solving simultaneously for velocity and pressure using a Newton–Raphson iterative method. The discrete variational formulation of this problem then reads

Find $(\mathbf{u}_h^{n+1}, p_h^{n+1}) \in V_h \times Q_h$ such that

$$\begin{aligned} \mathcal{R}_{\mathbf{u}} = & \int_{\Omega} \mathcal{G}_{\mathbf{u}} \cdot \mathbf{v}_h \, d\Omega + \int_{\Omega} 2\mu \nabla^S \mathbf{u}_h^{n+1} : \nabla \mathbf{v}_h \, d\Omega - \int_{\Omega} p_h^{n+1} \nabla \cdot \mathbf{v}_h \, d\Omega + \mathbf{f}_{\Gamma_h}^{n+1}(\mathbf{v}_h) + \\ & + \sum_{K \in \mathcal{T}_h} \tau_K \int_{\Omega_K} (\mathcal{G}_{\mathbf{u}} + \nabla p_h^{n+1}) \cdot \mathbf{u}_h^n \cdot \nabla \mathbf{v}_h + \sum_{K \in \mathcal{T}_h} \int_{\Omega_K} \delta_K \nabla \cdot \mathbf{u}_h^{n+1} \nabla \cdot \mathbf{v}_h \, d\Omega = 0 \quad (13) \end{aligned}$$

$$\mathcal{R}_p = \int_{\Omega} q_h \nabla \cdot \mathbf{u}_h^{n+1} \, d\Omega + \sum_{K \in \mathcal{T}_h} \int_{\Omega_K} \frac{\tau_K}{\rho} (\mathcal{G}_{\mathbf{u}} + \nabla p_h^{n+1}) \cdot \nabla q_h \, d\Omega = 0 \quad (14)$$

$\forall (\mathbf{v}_h, q_h) \in V_h \times Q_h$. In (13), the term $\mathcal{G}_{\mathbf{u}}$ is given by

$$\mathcal{G}_{\mathbf{u}} = \rho \left(\frac{\mathbf{u}_h^{n+1} - \mathbf{u}_h^n}{\Delta t} + \mathbf{u}_h^{n+1} \cdot \nabla \mathbf{u}_h^{n+1} - \mathbf{b}^{n+1} \right), \quad (15)$$

with Δt the time step and the stabilization parameters given by

$$\tau_K = c \left[4 \frac{\nu}{h^2} + 2 \frac{|\mathbf{u}_h|_{\infty}^n}{h} \right]^{-1}, \quad \delta_K = 2\mu + \rho |\mathbf{u}_h|_{\infty}^n h_K, \quad (16)$$

where c is an adjustable parameter.

Many authors introduce a regularized form of the Dirac delta function for the computation of $\mathbf{f}_{\Gamma_h}^{n+1}(\mathbf{v}_h)$ in (13) as proposed in Brackbill et al. (1992); Chang et al. (1996), therefore, the surface force is approximated as a volume force more or less concentrated around Γ depending on an adjustable regularization parameter. In our formulation, we *do not* use such regularizations and instead compute this term exactly, which precisely leads to sharp variations through the interface in the pressure field. Solving problem (13)–(14) accurately, requires the finite element spaces to be appropriately chosen, so as to accommodate discontinuities and/or kinks in the pressure and velocity fields. We first focus on how to improve the accuracy of the numerical approximation in several problems involving jumps in the pressure field, for which we introduce a *new* enrichment space.

3 THE NEW ENRICHMENT SPACE

Let us consider a finite element partition \mathcal{T}_h of Ω into simplices (triangles in 2D, tetrahedra in the 3D) and denote each element in the partition as Ω_K . The number of vertices per element is denoted by n_p (3 for triangles and 4 for tetrahedra). We consider the interface Γ_h composed of straight segments in 2D or planar facets in 3D. This interface is not conforming with the element edges. The element Ω_K can be divided into subelements Ω_K^+ and Ω_K^- . A typical element is shown in figure 1. An interface passing exactly through the nodes of the element leads to a degenerate case which is not considered here for brevity. In the three dimensional case, two situations have to be considered, since the reconstructed interface can be either a triangular or a quadrangular facet. In the discrete variational formulation presented above, the integrals over the elements are performed exactly by redefining the quadrature in the elements cut by. The velocity field is made up of continuous linear functions. For all the elements of \mathcal{T}_h that are not crossed by Γ_h the space Q_h is also made up of continuous linear functions. *The various possibilities to improve accuracy of the numerical approximation in problems involving jumps or kinks, consist in an enrichment or a modification of the finite element space Q_h only in those elements of \mathcal{T}_h crossed by Γ_h .*

The pressure field is written as

$$p_h = \sum_{J=1}^{n_P} P_J N_J + \sum_{J=1}^2 C_J M_J, \quad (17)$$

where the first sum corresponds to the standard degrees of freedom ($n_P = 3$ for linear triangles and 4 for linear tetrahedra) and the second sum corresponds to the additional enrichment degrees of freedom that are local to the element.

In order to build the enrichment functions, a requirement is that a constant solution on each fluid domain with a jump at the interface belong to the discrete space Q_h . To satisfy this requirement, we introduce two new enrichment functions that are linear on each subelement Ω_K^+ and Ω_K^- and discontinuous at Γ_h . We also require both functions to be zero at the nodes of the simplex. By inspection, we see that a possibility to define the enrichment functions is as follows:

$$M_1(\mathbf{x}) = (1 - S(\mathbf{x})) \chi^+(\mathbf{x}), \quad (18)$$

$$M_2(\mathbf{x}) = S(\mathbf{x}) \chi^-(\mathbf{x}), \quad (19)$$

where the function S is given in terms of the usual P_1 functions by

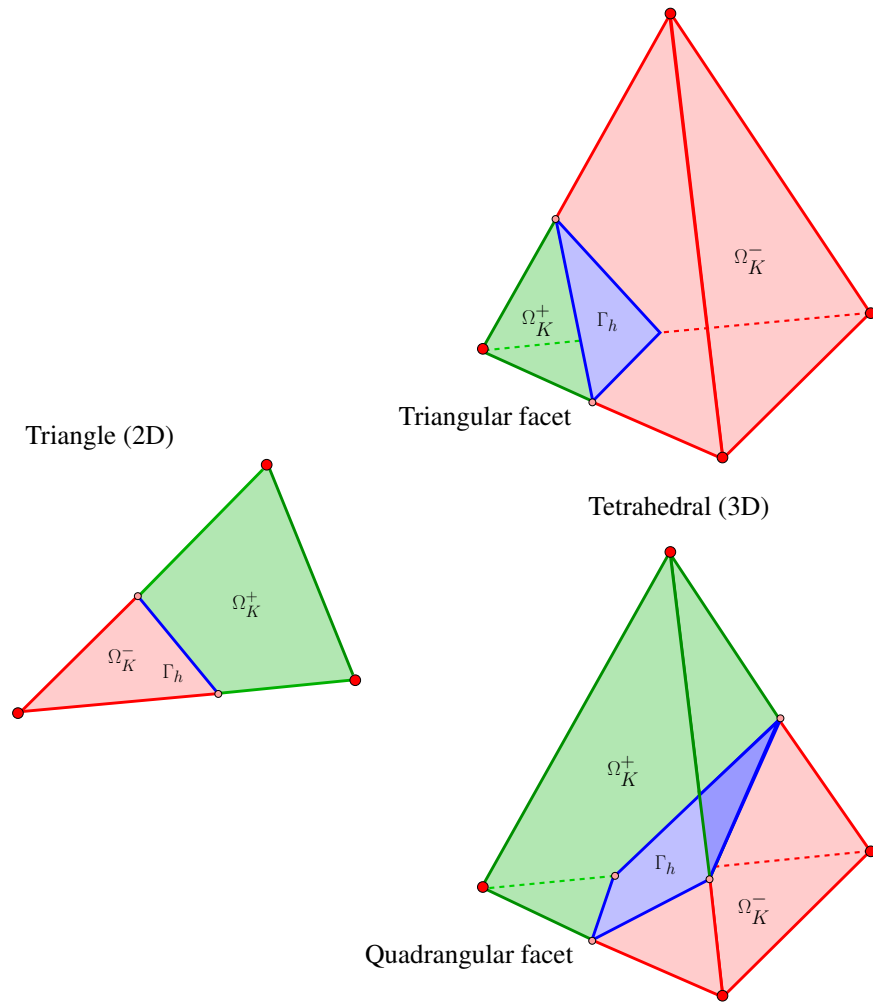


Figure 1: Typical element Ω_K and subelements Ω_K^+ and Ω_K^- and interface Γ_h .

$$S = \sum_{J \in \mathcal{J}^+} N_J(\mathbf{x}), \tag{20}$$

with $\mathcal{J}^+ = \{J \in \mathcal{J}, \mathbf{x}_J \in \Omega_K^+\}$, and χ^+ and χ^- the characteristic functions for the positive and negative sides. The pressure space thus has dimension $N_P + 2 N_E$, where N_P and N_E are the total number of nodes and elements respectively in \mathcal{T}_h . However, since the additional shape functions are local to each element crossed by the interface, they can be condensed prior to assembly and the size of the final linear system to be solved is the same as in the standard case. Note that this elimination can be done because the pressure is just involved in linear terms of the problem.

In figure 2 the enrichment functions for a typical triangular element are shown. In the left part of the figure, the two functions are shown separately and in the right part they are plot together just for illustrative purposes.

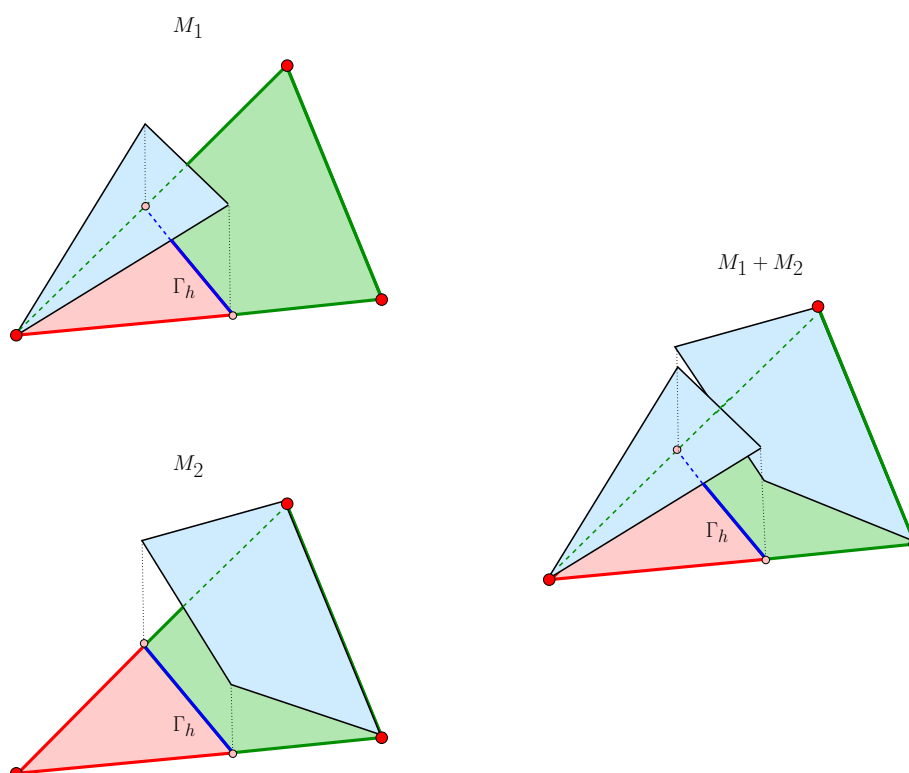


Figure 2: New enrichment functions in a typical triangular element. In the left, the two functions are drawn separately and in the right, the two functions are drawn together just for illustrative purposes.

4 NUMERICAL EXAMPLES

4.1 An academic example

We consider the computational domain $[0, 1] \times [0, 1]$ split by the straight horizontal interface $x_2 = a$ separating regions with different values for the parameters μ_1 and μ_2 . The interface is kept fixed. The parameter ρ is assumed the same for both regions. Considering the following linear field \mathbf{u}

$$u_1(x_1, x_2) = 1 - x_1, \quad (21)$$

$$u_2(x_1, x_2) = x_2, \quad (22)$$

assuming $\mathbf{b} = 0$, it can be easily found that the exact solution for the field p is quadratic on each region, with a jump at the interface due to the difference between μ_1 and μ_2 and is given by

$$p(x_1, x_2) = \rho \left(x_1 - \frac{1}{2}(x_1^2 + x_2^2) \right) + 2(\mu_1 - \mu_2)\mathcal{H}(a - x_2) \quad (23)$$

where $\mathcal{H}(a - x_2) = 1$ if $x_2 < a$ and zero otherwise. The indeterminacy of the pressure in the simulations is again removed by imposing $p(1, 1) = 0$ instead of setting the average to zero. In order to reproduce this exact solution, the velocity field given by (21)–(22) is imposed at the boundaries.

The problem is solved with $\rho = 10$, $\mu_1 = 5$ and $\mu_2 = 1$ and $a = 0.5$ using the classical P_1 -conforming pressure space, the new enrichment space and the space of Ausas et al. (2010a). A sequence of unstructured meshes was built, of which the first one is shown in Fig. 3. To this

mesh, which consists of 1104 triangles, we assign a mesh size of $h = 0.0055$. The following meshes in the sequence are built by subdivision of each triangle into four equal triangles. We measure the velocity error in the $H^1(\Omega)$ -norm and the pressure error in the $L^2(\Omega)$ -norm as function of h . The results of the convergence analysis are displayed in Fig. 4 and 5. Results for the new enrichment space exhibit in this case a much smaller error (more than one order of magnitude) than results for the space of Ausas et al. (2010a) in both pressure and velocity. Also, for the meshes considered, we observe a better convergence order of the new enrichment space, equal to h^2 for pressure and $h^{\frac{5}{2}}$ for velocity.

In Fig. 6, cuts of the field p at $x_1 = 0.5$ are compared, where the better behavior near the interface using the new enrichment space as compared to the classical P_1 -conforming space is noticed. Note that the case with $\rho = 0$ corresponds to a constant solution for the field p on each fluid, with a jump at the interface of magnitude $2(\mu_1 - \mu_2)$. This solution belongs to the finite element spaces when either, the new enrichment space or the space of Ausas et al. (2010a) are used.

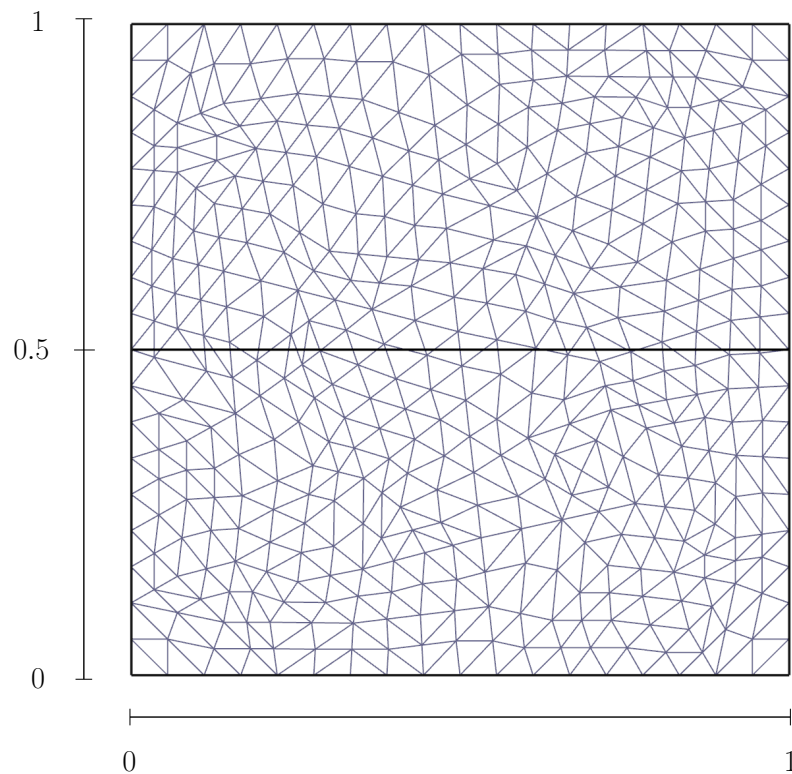


Figure 3: Mesh for the academic problem convergence study, with 1104 elements and $h = 0.01$.

4.2 A 3D example: Rising bubbles

In the previous academic example the interface Γ was fixed. Now, we aim to show the good behavior of the new enrichment space in a more complex situation including the transport of the interface. In this article a level set formulation is used, in which the interface is the zero set of a continuous scalar function ϕ , i.e.

$$\Gamma = \{\mathbf{x} \in \Omega, \phi(\mathbf{x}) = 0\}. \quad (24)$$

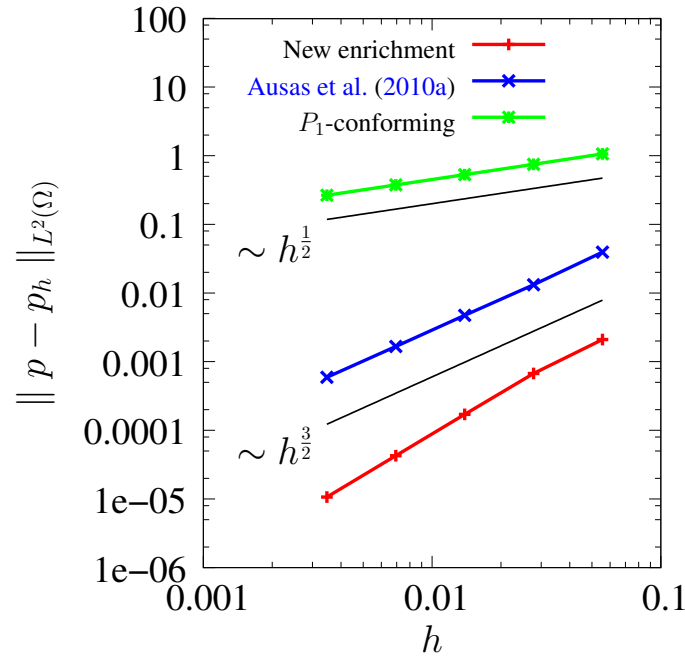


Figure 4: Error norm for the pressure field, showing the convergence rates for the academic example.

The function ϕ is transported according to

$$\frac{\partial \phi}{\partial t} + \mathbf{u} \cdot \nabla \phi = 0. \quad (25)$$

which is solved together with the velocity and pressure fields using a SUPG method (see Hughes (1987)) by adding the following to (13)–(14)

Find $\phi_h^{n+1} \in W_h$ such that

$$\sum_{K \in \mathcal{T}_h} \int_{\Omega_K} \left(\frac{\phi_h^{n+1} - \phi_h^n}{\Delta t} + \mathbf{u}_h^{n+1} \cdot \nabla \phi_h^{n+1} \right) (w_h + \tilde{\tau}_K \mathbf{u}_h^{n+1} \cdot \nabla w_h) d\Omega = 0 \quad (26)$$

$\forall w_h \in W_h$. The discrete space W_h is made up of continuous linear functions. The stabilization parameter $\tilde{\tau}_K$ is taken as

$$\tilde{\tau}_K = \frac{\tilde{c} h}{2 |\mathbf{u}_h|_\infty}, \quad (27)$$

With this formulation, we study the rise of a buoyant bubble. This problem has been solved many times before (see e.g. Marchandise et al. (2007) and references therein). We assume a bubble with density $\rho_1 = 10^{-3}$ and viscosity μ_1 in a quiescent liquid with density $\rho_2 = 1$ and viscosity μ_2 in the computational domain $\Omega = (0, 2.25) \times (0, 2.25) \times (0, 4)$. At the initial time the diameter of the bubble is 1 and is placed at the position (1.125, 1.125, 1). The gravity g is taken to -10 . We consider two different regimes corresponding to parameters given in table 1. The first case, is labeled as spherical regime. In this case surface tension effects are dominant and the bubble's shape remains approximately spherical during its evolution. The second case is labeled as skirted regime. In this case, surface tension effects are less important and the bubble suffers a larger deformation during its evolution.

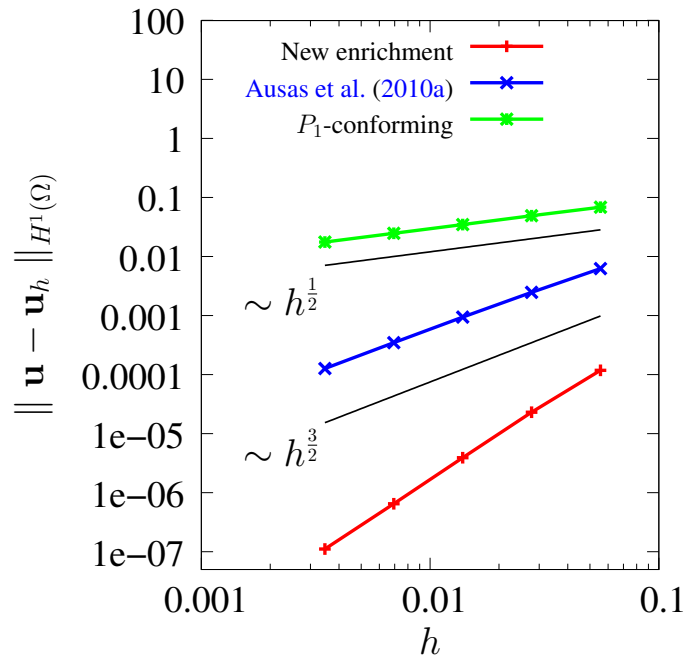


Figure 5: Error norm for the velocity, showing the convergence rates for the academic example.

Table 1: Physical parameters for the two regimes considered for the rise of a buoyant bubble in 3D.

Regime	ρ_1	μ_1	ρ_2	μ_2	γ
Spherical	10^{-3}	3×10^{-4}	1	0.3	10
Skirted	10^{-3}	10^{-4}	1	0.1	0.1

The discrete variational formulation with the new enrichment space was included into a general purpose in-house code which is described elsewhere (see Ausas (April, 2010)). The level set function is periodically reinitialized by means of a mass-preserving redistancing scheme (see Mut et al. (2006); Ausas et al. (2010b)) to keep its distortion under control. For this problem, the finite element mesh used consists of 1,511,016 tetrahedra and the time step is taken equal to 5×10^{-4} for both regimes.

For the spherical regime, shown in figure 7 is the interface shape at times $t = 0, 0.375$ and 0.75 . The bubbles are painted with the velocity magnitude. It is evident from the figure the benefits regarding mass conservation when the new enrichment space is used with respect to the classical P_1 -conforming space. In the former case, a 2% of the bubble’s mass is lost at the final time shown in the figure against a 60% in the case without enrichment.

For the skirted regime, to better appreciate the benefits of the new enrichment space, we plot in figure 8 the bubbles at different times together. We observe the typical cap shape attained by the bubble. For the case using the new enrichment, the bubble is plotted in the left side, in red, while for the case using the classical P_1 -conforming space, the bubble is plotted in the right side, in blue. The mass lost is 0.14% in the first case and 15% in the second one, clearly evidencing the benefits of the new pressure space. For both regimes, similar results to those corresponding to the new enrichment are obtained if the space of Ausas et al. (2010a) is used instead.

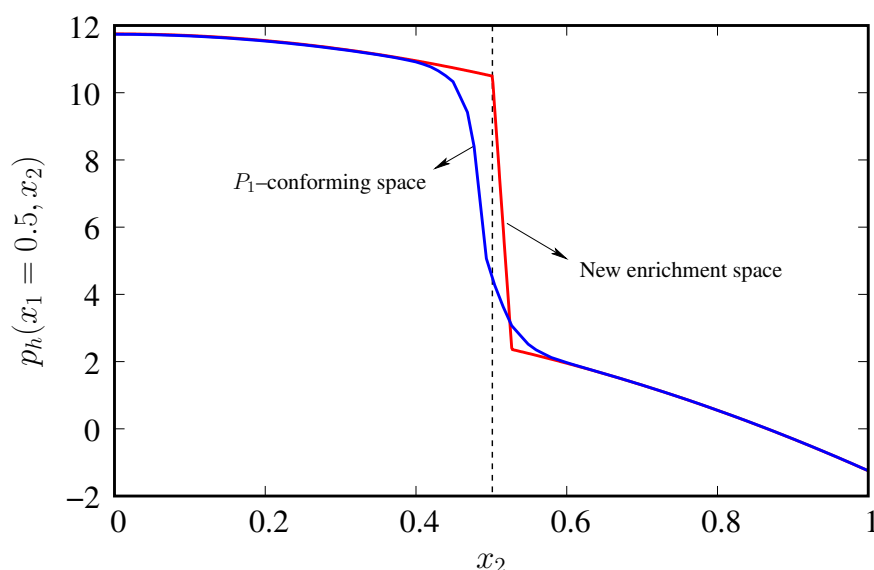


Figure 6: Section at $x_1 = 0.5$ of the field p for the academic example using the new enrichment space and the P_1 -conforming space.

5 SUMMARY

In this article a new pressure space has been introduced to accommodate jumps in the pressure field at immersed interfaces in two-phase flows. The new space incorporates two statically condensable degrees of freedom per element crossed by the interface. The enrichment space has been compared to other pressure spaces. In the classical Couette flow problem with a singular force the error norms for pressure and velocity, showed very similar results as in the case with the space of Ausas et al. (2010a). For the extensional flow problem, the error norms resulted in more than one order of magnitude smaller errors and a better convergence order for the new enrichment space as compared to the space of Ausas et al. (2010a). The new enrichment space has also been tested in a 3D problem involving the rising of a bubble in a quiescent liquid considering two different physical regimes. In this case also the new enrichment space exhibited excellent results regarding mass conservation as compared to the classical P_1 -conforming space.

ACKNOWLEDGMENTS

The authors acknowledge partial support from FAPESP (Brazil), CNPq (Brazil). This research was carried out in the framework of INCT-MACC, Ministério de Ciência e Tecnologia, Brazil.

REFERENCES

- Adalsteinsson D. and Sethian J. A fast level set method for propagating interfaces. *J. Comput. Phys.*, 118:269–277, 1995.
- Ausas R. *Numerical simulation in two-phase immiscible flows with applications in hydrodynamic lubrication*. Ph.D. thesis, Engineering, Instituto Balseiro., April, 2010.
- Ausas R. and Buscaglia G. A PDE-based velocity extrapolation method for the transport of the level set function in two phase liquid-gas flows. *Serie Mecánica Computacional*, XXIX:3189–3206, 2010.
- Ausas R., Sousa F., and Buscaglia G. An improved finite element space for discontinuous

- pressures. *Comput. Methods Appl. Mech. Engrg.*, 199:1019–1031, 2010a.
- Ausas R.F., Buscaglia G.C., and Dari E.A. A geometric mass-preserving redistancing scheme for the level set function. *Int. J. Num. Meth. Fluids*, 65:989–1010, 2010b.
- Baiges J., Codina R., and Coppola-Owen H. The fixed-mesh ale approach for the numerical simulation of floating solids. *International Journal for Numerical Methods in Fluids*, pages n/a–n/a, 2010. ISSN 1097-0363. doi:10.1002/flid.2403.
- Bänsch E. Finite element discretization of the Navier–Stokes equation with a free capillary surface. *Numer. Math.*, 88:203–235, 2001.
- Belytschko T., Moës N., Usui S., and Parimi C. Arbitrary discontinuities in finite elements. *Int. J. Numer. Meth. Engrg.*, 50:993–1013, 2001.
- Brackbill J.U., Kothe D.B., and Zemach C. A continuum method for modeling surface tension. *J. Comput. Phys.*, 100:335–354, 1992.
- Buscaglia G. and Agouzal A. Interpolation estimate for a finite element space with embedded discontinuities. *IMA Journal of Numerical Analysis*, *accepted*, 2011.
- Carrica P., Wilson R., and Stern F. An unsteady single–phase level set method for viscous free surface flows. *Int. J. Numer. Meth. Fluids*, 53:229–256, 2007.
- Chang Y., Hou T., Merriman B., and Osher S. A level set formulation of eulerian capturing methods for incompressible fluid flows. *J. Comput. Phys.*, 124:449–464, 1996.
- Chessa J. and Belytschko T. A extended finite element method for two–phase fluids. *Journal of Applied Mechanics*, 70:10–17, 2003.
- Codina R. A stabilized finite element method for generalized stationary incompressible flows. *Comput. Methods Appl. Mech. Engrg.*, 190:2681–2706, 2001.
- Coppola-Owen A.H. and Codina R. Improving eulerian two–phase flow finite element approximation with discontinuous gradient pressure shape functions. *Int. J. Numer. Meth. Fluids*, 49:1287–1304, 2005.
- Cruchaga M., Calentano D., and Tezduyar T. A moving Lagrangian interface technique for flow computations over fixed meshes. *Comput. Methods App. Mech. Engrg.*, 191:525–543, 2001.
- Cummins S., Francois M., and Kothe D. Estimating curvature from volume fraction. *Computers and Structures*, 83:425–434, 2005.
- Dettmer W., Saksono P., and Perić D. On a finite element formulation for incompressible Newtonian fluid flows on moving domains in the presence of surface tension. *Commun. Numer. Meth. Engrg.*, 19:659–668, 2003.
- Di Pietro D., Lo Forte S., and Parolini N. Mass preserving finite element implementations of the level set method. *Applied Numerical Mathematics*, 56:1179–1195, 2006.
- Enright D., Fedkiw R., Ferziger J., and Mitchell I. A hybrid particle level set method for improved interface capturing. *Computers and Structures*, 83:479–490, 2002.
- Enright D., Losasso F., and Fedkiw R. A fast and accurate semi-Lagrangian particle level set method. *Computers and Structures*, 83:479–490, 2005.
- Fries T.P. and Belytschko T. The intrinsic XFEM: a method for arbitrary discontinuities without additional unknowns. *Int. J. Numer. Meth. Engrg.*, 68:1358–1385, 2006.
- Ganesan S., Matthies G., and Tobiska L. On spurious velocities in incompressible flow problems with interfaces. *Comput. Methods Appl. Mech. Engrg.*, 196:1193–1202, 2007.
- Gross S. and Reusken A. An extended pressure finite element space for two-phase incompressible flows with surface tension. *J. Comput. Phys.*, 224:40–58, 2007a.
- Gross S. and Reusken A. Finite element discretization error analysis of a surface tension force in two-phase incompressible flows. *SIAM J. Numer. Anal.*, 45:1679–1700, 2007b.
- Gueyffier D., Lie J., Nadim A., Scardovelli R., and Zaleski S. Volume–of–fluid interface track-

- ing with smoothed surface stress methods for three-dimensional flows. *J. Comput. Phys.*, 152:423–456, 1999.
- Hirt C., Amsden A., and Cook J. An Arbitrary-Lagrangian-Eulerian computing method for all flow speeds. *J. Comput. Phys.*, 14:227–253, 1974.
- Hirt C. and Nichols H. Volume of fluid (VOF) methods for the dynamics of free boundaries. *Applied Numerical Mathematics*, 39:201–225, 1981.
- Hughes T. Recent progress in the development and understanding of SUPG methods with special reference to the compressible Euler and Navier–Stokes equations. *Int. J. Numer. Meth. Fluids*, 7:1261–1275, 1987.
- Hughes T., Liu W., and Zimmermann T. Lagrangian–Eulerian finite element formulation for incompressible viscous flows. *Comput. Meth. Appl. Mech. Engrg.*, 29:329–349, 1981.
- Idelsohn S., Mier-Torrecilla M., and Oñate E. Multi-fluid flows with the particle finite element method. *Comput. Methods Appl. Mech. Engrg.*, In press, 2009.
- Idelsohn S., Oñate E., and Del Pin F. The particle finite element method: A powerful tool to solve incompressible flows with free-surfaces and breaking waves. *Int. J. Num. Meth. Engrg.*, 61:964–989, 2004.
- Jiang G.S. and Peng D. Weighted ENO schemes for Hamilton-Jacobi equations. *SIAM J. Sci. Comput.*, 21:2126–2144, 2000.
- Kothe D., Rider W., Mosso S., Brock J., and Hochstein J. Volume tracking of interfaces having surface tension in two and three dimensions. *AIAA*, 0859, 1996.
- Löhner R., Yang C., and Oñate E. On the simulation of flows with violent free surface motion. *Comput. Methods Appl. Mech. Engrg.*, 195:5597–5620, 2006.
- Marchandise E., Geuzaine P., Chevaugéon N., and Remacle J.F. A stabilized finite element method using a discontinuous level set approach for the computation of bubble dynamics. *J. Comput. Phys.*, 225:949–974, 2007.
- Marchandise E., Remacle J.F., and Chevaugéon N. A quadrature-free discontinuous Galerkin method for the level set equation. *J. Comput. Phys.*, 212:338–357, 2006.
- Minev P.D., Chen T., and Nandakumar K. A finite element technique for multifluid incompressible flow using Eulerian grids. *J. Comput. Phys.*, 187:255–273, 2003.
- Mut F., Buscaglia G., and Dari E. New mass-conserving algorithm for level set redistancing on unstructured meshes. *Journal of Applied Mechanics*, 73:1011–1016, 2006.
- Osher S. and Fedkiw R. Level set methods: An overview and some recent results. *J. Comput. Phys.*, 169:463–502, 2001.
- Popinet S. and Zaleski S. A front-tracking algorithm for accurate representation of surface tension. *Int. J. Numer. Meth. Fluids*, 30:775–793, 1999.
- Reusken A. Analysis of an extended pressure finite element space for two-phase incompressible flows. *Comput. Visual. Sci.*, 11:293–305, 2008.
- Sethian J. Evolution, implementation and application of level set and fast marching methods for advancing fronts. *J. Comput. Phys.*, 169:503–555, 2001.
- Shu C. and Osher S. Efficient implementation of essentially non-oscillatory shock-capturing schemes. *J. Comput. Phys.*, 77:439–471, 1988.
- Strain J. Semi-Lagrangian methods for level set equations. *J. Comput. Phys.*, 151:498–533, 1999a.
- Strain J. Tree methods for moving interfaces. *J. Comput. Phys.*, 151:616–648, 1999b.
- Sweby P. High resolution schemes using flux limiters for hyperbolic conservation laws. *SIAM J. Numer. Anal.*, 21:995–1011, 1984.
- Unverdi S. and Tryggvason G. A front-tracking method for viscous, incompressible, multi-

fluid flows. *J. Comput. Phys.*, 100:25–37, 1992.

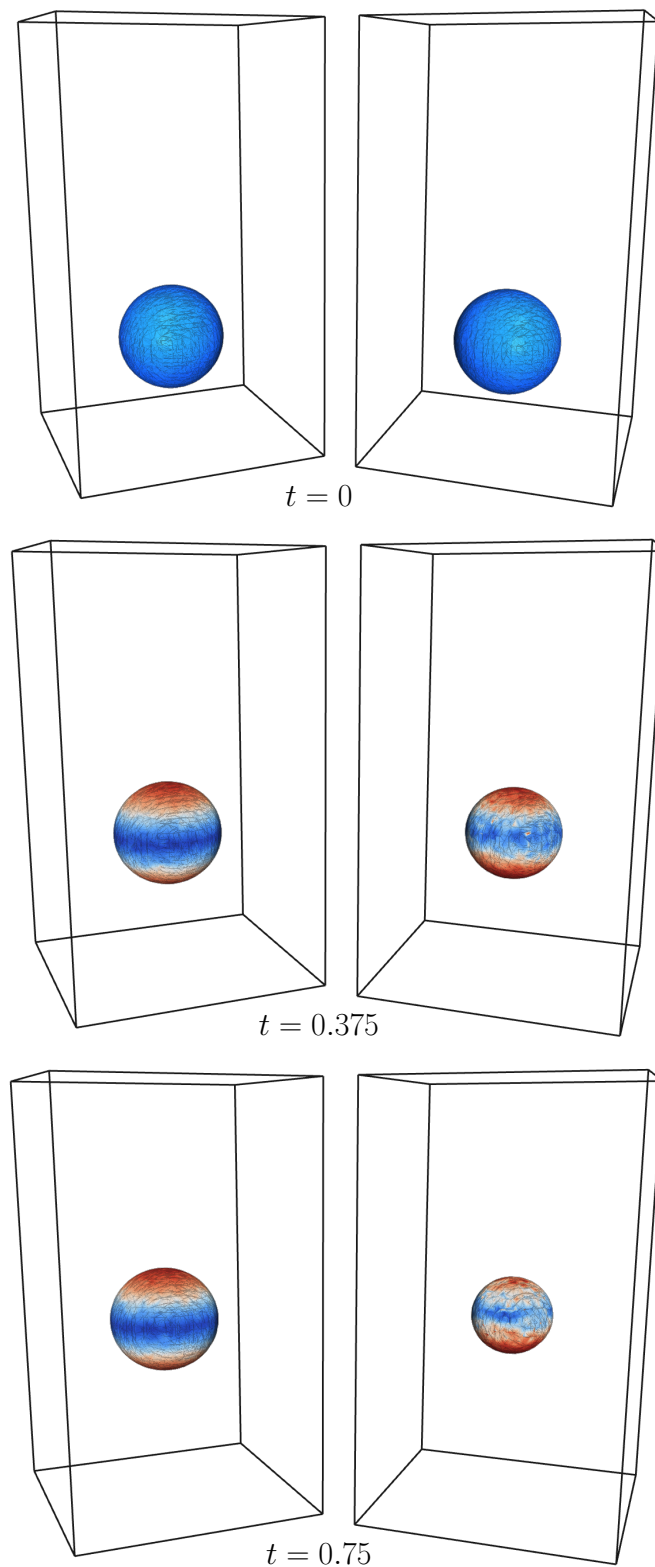


Figure 7: Comparison of the three dimensional rising bubble at different times for the spherical regime, using the new enrichment space (left) and the classical P_1 -conforming space (right). For times 0.375 and 0.75, the maximum of the colour scale corresponds to 1.3 (red) and the minimum to 0.02 (blue).

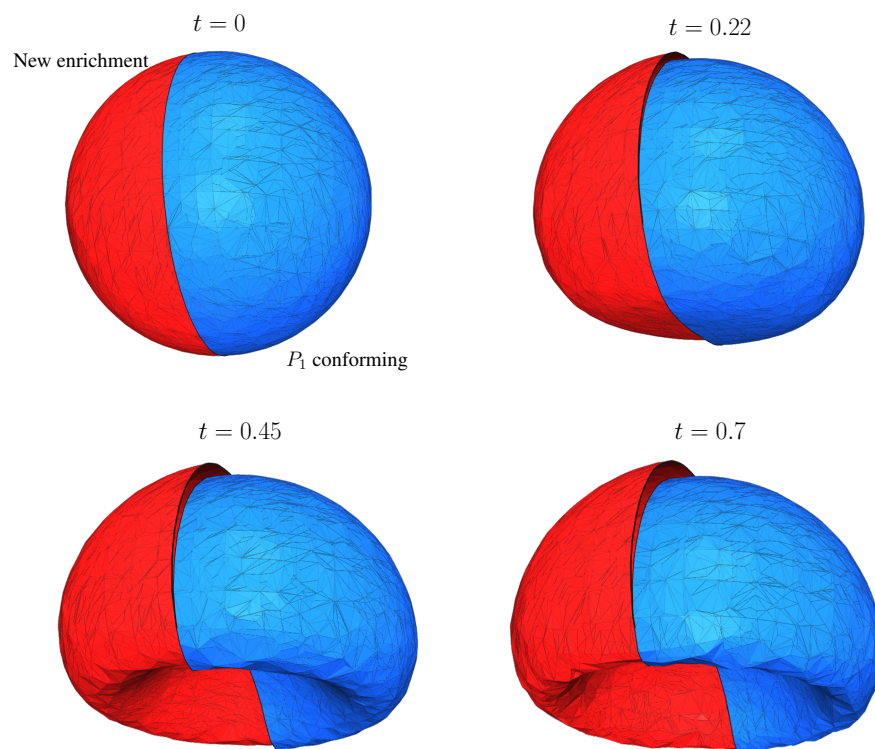


Figure 8: Comparison of the three dimensional rising bubbles at different times for the skirted regime, using the new enrichment space (left, red) and the classical P_1 -conforming space (right, blue).